Variations in discharge from the Qilian mountains, northwest China, and its effect on the agricultural communities of the Heihe basin, over the last two millennia

Akiko Sakai · Mitsuyuki Inoue · Koji Fujita · Chiyuki Narama · Jumpei Kubota · Masayoshi Nakawo · Tandong Yao

Abstract   Over the last two millennia, agricultural land in the Hei river basin, northwest China, has been subjected to a series of significant droughts and flood events. These documented hydrological events were compared to estimates of fluvial and fluvioglacial discharge from the mountains. Areal extents of glaciers are important for validation as water mass remaining in mountain area, although glacier area occupied only about 1.5 % at present in this high mountain area. These glacier mass balance and discharge estimates, calculated using proxy data, appear reasonable, as the total maximum glacier area during the little ice age (LIA) was comparable to the maximum glacier area deduced from the positions of terminal moraines. The precise timing of the glacier area maximum during the LIA in the Qilian mountains is unknown. However, variations in the calculated glacier area

A. Sakai (✉) · K. Fujita
Graduate School of Environmental Studies, Nagoya University, Furo-cho, Chikusa-ku,
Nagoya, Aichi, Japan
e-mail: shakai@nagoya-u.jp

K. Fujita
e-mail: cozy@nagoya-u.jp

M. Inoue
Ritsumeikan University, Kyoto, Japan
e-mail: zhulan@fc.ritsumei.ac.jp

C. Narama · J. Kubota
Research Institute for Humanity and Nature, Kyoto, Japan
e-mail: narama@chikyu.ac.jp

J. Kubota
e-mail: jkubota@chikyu.ac.jp

M. Nakawo
National Institutes for the Humanities, Tokyo, Japan
e-mail: nakawo@nihu.jp

T. Yao
Institute of Tibet Plateau Research, Chinese Academy of Science, Beijing, People's Republic of China
e-mail: tdyao@itpcas.ac.cn

suggest that glacier extent reached a maximum between 1520 and 1690 CE. A number of the historical drought events occurred during periods of reduced discharge from the mountains, and, conversely, flood events tended to coincide with an increase in discharge from glaciers. Historical documents record five multi-year droughts in the basin between 1200 and 2000 CE. The modelling of the fluctuating pattern of fluvial and fluvioglacial discharge implies that at least two drought events were anthropogenically driven. Furthermore the reasons for the presence or absence of drought events are considered based on continuous discharge fluctuation and water demands of each ages, that can be estimated from analysing intermittent historical documents.

Keywords Glacier · Discharge · Drought · Arid region · Precipitation

Introduction

In the arid regions of China, precipitation in the surrounding mountain ranges plays a significant role in providing water for the desert and oasis cities. The Heihe basin of northwest China is one such arid region (Fig. 1a), that can be divided into three parts: upper, middle, and lower. The Qilian mountains form the upper, glaciated reaches. In the

Fig. 1 a Location map showing the Heihe Basin, Qilian Mountains, and tree-ring sample sites at Dulan. Thick solid lines represent mountain ranges. **b** The three basins studied are part of the mountain region of the Heihe Basin, and have been divided into 0.5° latitude/longitude grid squares
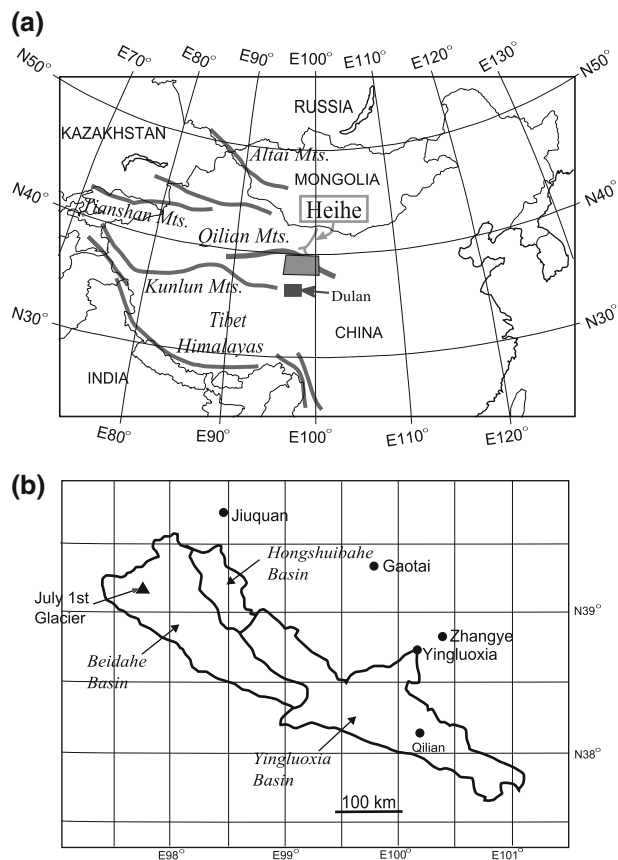
middle zone, at the northern foot of the Qilian mountains, are the oasis cities of Zhangye and Jiuquan. Finally, the vast Gobi desert occupies the lower reaches of the basin, across which the Heihe flows northwards before debouching into terminal lakes.

At high elevations, in the mountainous zones to the south of the Gobi desert, relatively large amounts of precipitation (300–500 mm yr^{-1}) occur. In contrast, there is little precipitation (30–50 mm yr^{-1}) downstream in the desert zones to the north (Wang and Cheng 1999). Most precipitation in the desert zone quickly evaporates; consequently, water is unable to accumulate as either groundwater or in rivers. Therefore, precipitation stored in the nearby mountain glaciers is an important water resource (Wang and Cheng 1999), and melt water from glaciers and snow in these mountains has long provided an important source of drinking water and a means of irrigation for people living in the desert and oasis cities. However, by the latter part of the 19th century, runoff in some major tributaries of the Heihe had diminished due to an increase in the irrigation area (Wang and Cheng, 1999), resulting in adverse environmental impacts such as seasonal water shortage affecting farming in the lower reaches of the Qilian mountains.

Endo et al. (2005) have summarised the history of the lower reaches of Heihe basin based on analysis of lake sediments as follows. The lower reaches can be divided into two main parts; namely, the Juyan delta (old Juyan lake) and the Ejina delta (Gashon Nor and Sogo Nor) (Fig. 2). The Juyan lake has expanded greatly since 7500 BP. However, in 300 CE, the water level of old Juyan lake dropped, as the river channel shifted gradually westwards towards the Ejina delta, due to the development of sand dunes on the Juyan delta. In contrast, river water has flowed into Sogo Nor since 2500 BP, and Sogo Nor and
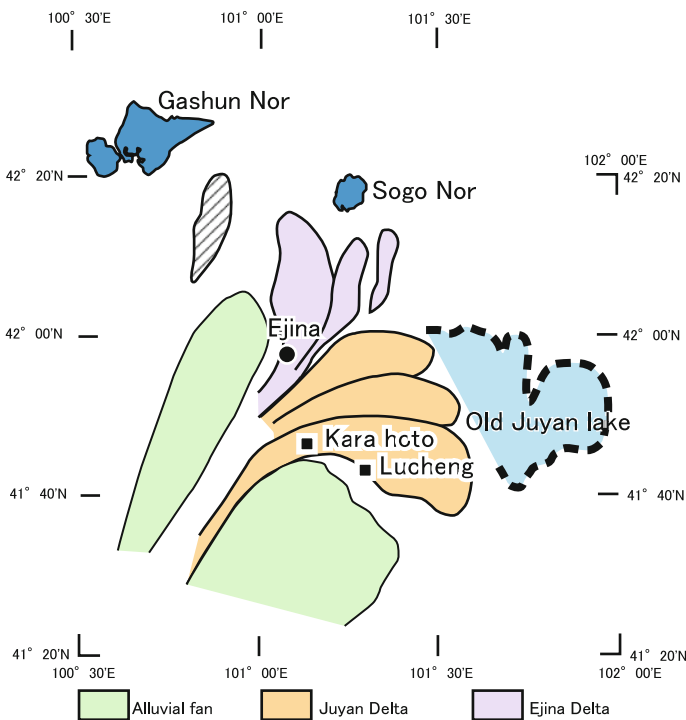

Fig. 2 Lakes and deltas of the lower reaches of the Hei River Basin (modified from Fig. 1 in Endo et al. 2005)

Gashon Nor became large lakes in 1200 CE. In this way, the hydrological conditions of the lower reaches has been changed significantly due to river channel change in the Heihe basin, changes that are described in the next section.

The upper reaches of the Heihe basin are comprised of the Yingluoxia, Beidahe, and Hongshuibahe basins (Fig. 1b). Sakai et al. (2010) established a method for calculating discharge from the Yingluoxia basin, the largest basin in the Heihe catchment. Changes in runoff from the Qilian mountains, in response to climate change, have been simulated by Kang et al. (1999) using the Hydrologiska Byråns Vattenbalansavdelning (HBV) model. They concluded that the annual discharge from a mountainous area would fall if the annual temperature increased by 0.5 °C, even if precipitation levels remained constant, due to the increase in evaporation.

Numerical simulations of a number of glaciers have been developed in an attempt to model their behaviour over the past few decades and to predict their response to future changes (e.g., Greuell 1992; Raper et al. 1996; Oerlmans 1997; Schmeits and Oerlemans 1997; Zuo and Oerlemans 1997; Smedt and Pattyn 2003; Linderholm and Jansson 2007; Yamaguchi et al. 2008). These researchers reconstructed past variations in glacier length, or glacier mass balance, and discussed the sensitivity of glacier length to changes in precipitation; however, they did not attempt to reconstruct variations in glacier area, or evaluate variations in discharge from the glaciers. Here, the discharge from the three basins of the Hei river system are calculated for the last two millennia, using proxies for temperature and precipitation data. These discharge data are then compared with the historical records to see when hydrological events coincide. We discuss the similarities between the two data sets, and it is demonstrated that the method can be used for the analysis of historical flooding and drought events at northwest China including the Heihe basin.

Historical data

Nakawo (2011) summarized historical records such as '*Juyan Hanjian*', '*Suishu*' and '*Tongdian*' in relation to climate change and the water environment in the Heihe basin. The water environment is briefly outlined in the following paragraphs.

Few historical documents survive from the later Han Dynasty (25–220 CE). However, an ancient inhabited site and irrigation network, on the Juyan delta, was identified from an analysis of a Corona satellite image. Dating evidence based on pottery finds, and C-14 dating of charcoal, indicates that irrigated agriculture was active two period on the Juyan delta, one during the Han period, and the other during the Xixia-Yuan period (1032–1368 CE). And a large irrigation system was already in existence over 2000 years ago (Endo et al. 2005; Nakawo 2011). During the Wei, Jin, and the southern and northern Dynasties (220–589 CE), the old Juyan lake contracted rapidly around 300 CE, because water from the Hei river had started to flow into the present-day Sogo Nor (Endo et al. 2005). The agricultural land of the Juyan delta was then abandoned but was later colonised by a nomadic people. Four droughts occurred along the Hexi Corridor during this period (271, 369, 399, and 405 CE) (Three Kingdoms Period). In the Sui period (581–618 CE), there is only one reference to the Hexi Corridor in '*Suishu*' (605–616 CE), which states that: 'There is a lot of land, but there are relatively few people.' The document also records some small-scale resettlement of frontier soldiers in the region at this time.

In the Tang period (618–907 CE), an inspection report (opinion by Chen Zi'ang) from 685 CE covering the middle reaches of the Hei at Ejina and Ganzhou (present-day Zhangye), stated that: 'irrigated agriculture is carried out only at Ganzhou (present-day Zhangye), and this is the breadbasket of the Hexi Corridor'. There are also descriptions in

the 'opinion by Chen Zi'ang' of the lower reaches: 'Juyan lake contact with Hei river at Ejina. Agricultural land expands in the form of grass land, where stock farming was possible. There is a lot of fish and salt in the lake and river.' While Endo et al. (2005) found that the old Juyan lake was already much reduced in size by 300 CE. 'The opinion by Chen Zi'ang' also suggested that in 685 CE, following three years of drought on the Mongol plateau, a large number not quantified of displaced people had arrived in Ejina.

During the Sung period (960–1279 CE), east China was governed by Sung, however, the Hei river region, which was mainly occupied by the Tangut people, was governed by Xixia (1038–1227 CE). An encyclopaedia ('Shengli Yihai'), published by Xixia in 1182 CE, contains descriptions of the glaciated mountain regions and of the lifestyle of the inhabitants: 'the local people cultivate the land using irrigation and also keep animals, such as sheep and horses'. The 'Dafo-si' temple in present-day Zhangye, built during the Xixia period, contains a stone monument known as 'Heishuiqiao-bei', which dates to 1176 CE and describes how the Hei river caused flooding every year. In the lower reaches, stock farming was dominant with little arable land in use; however, during the Xixia period, an increased use of irrigation allowed an expansion of crop cultivation, and this was accompanied by a phase of urban development that included 'Khara Khoto' (Black city) and 'Lücheng (Green city)'(Fig. 2). Dating of fragments of wheat and charcoal recovered from a former water channel indicate that this period of expansion occurred between 1160 and 1185 CE (Endo et al. 2005). However, Diatom analysis of lake sediment from Gashun Nor indicates that by 1200 CE the main channel of the Hei river had switched course away from the Juyan delta to the Ejina delta, and flowed into Gashun Nor following the development of a sand dune (Endo et al. 2005). Consequently, the cultivated land on the Juyan delta was deprived of water.

The subsequent Yuan period (1271–1368 CE) was previously believed to have been dominated by a nomadic people; however, there were significant attempts to increase the amount of agricultural land under cultivation. Farmer–soldiers were settled at Zhangye in 1281 CE CE, and then at Ejina in 1285 and 1288 CE; in addition, the sophisticated farming method known as 'Outian-fa', which involves the construction of irrigation systems, was in use across the country. Traces of 'Outian-fa' were found near the Green city, on the Juyan delta (Sohma et al. 2007). Furthermore, the irrigation systems of the Yuan Dynasty allowed for recycling of the water, in an attempt to adapt to this period of relative water shortage (Endo et al. 2005), unlike those built during the wetter Han Dynasty, when recycling was not required. Documents excavated from Khara Khoto describe how: 'there is very little water in the Hei river at present', indicating that the lower reaches yielded little available water at this time. In addition, there are records of the drought at Ejina in 1299 and 1331 CE; water shortages were also recorded in 1326 CE. Three historical documents (Honil Kangni Yoekdae Gukdo Chido (map of integrated lands and regions of historical countries and capitals, written in 1402 CE); Yong Daji (local gazetteer of Xaanxi Province written in 1522 CE); Qinbianjilüe (local gazetteer of northwestern border written in 1684 CE); show that the area occupied by the old Juyan lake had dramatically reduced, and that the lake had divided into three smaller lakes by the 13–14th centuries. The depth of these small lakes was only 1–2 m; such that, they were swamp-like (Nakawo 2011).

Beginning in 1390 CE, during the Ming Dynasty (1368–1644 CE), the amount of irrigated agricultural land had expanded dramatically in the middle reaches of the Hei basin (at Zhangye and Jiuquan) to compensate for the loss of cultivated land on the Juyan delta (Fig. 3). In the Ming period, a number of droughts were recorded, but C-14 dating shows that the Ejina delta developed around 1350–1400 CE, following a flood at the point where Sogo Nor and Gashun Nor divided (Endo et al. 2005). In the lower reaches, further
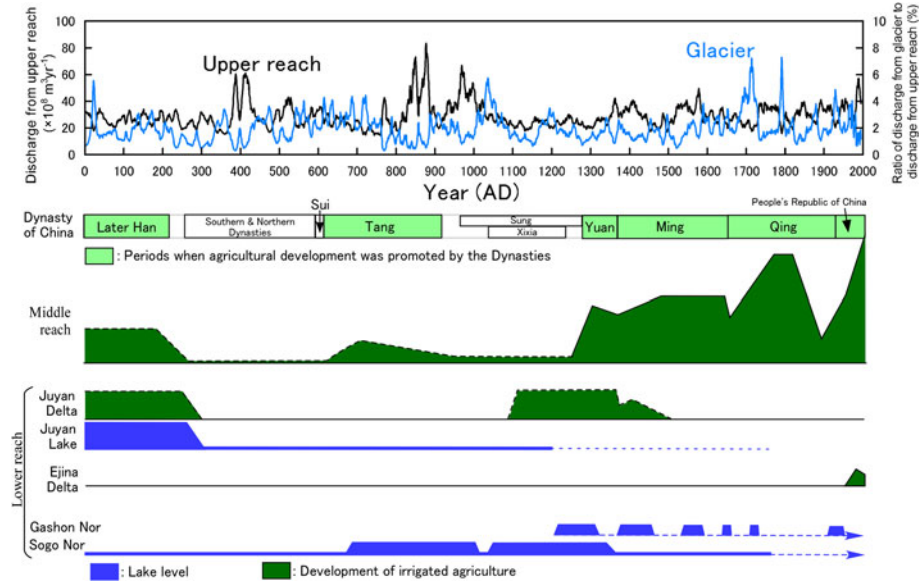
Fig. 3 Summary of the hydrological environment of the Hei River Basin, comprising the calculated discharge from the mountain area, the proportion of discharge originating from the glacier, agriculture activity in the middle and lower reaches (Nakawo 2011), and the area of the terminal lakes in the lower reaches. The locations of the deltas and lakes in the lower reaches are shown in Fig. 2. Also shown are changes in the levels of Gashun Nor and Old Juyan Lake (Endo et al. 2007), and of Sogo Nor (Mischke 2001)

settlement of ex-military took place on the Ejina delta in 1406 CE, and C-14 dating of plant remains found in the wall of a water channel near Lücheng confirm that irrigation channels were still being used in 1413 CE (Endo et al. 2005). However, in 1475 CE, Tamarix cones and plants covered the irrigation channel developed near Khara Khoto and Lücheng (Fig. 2), which indicates that cultivation was abandoned at the time because Tamarix would not have grown if the water channel was being actively maintained (Endo et al. 2005).

By 1712 CE, during the Qing period (1644–1912 CE), there were considerable problems and conflicts associated with the use of water for irrigation, and river water did not reach the lower reach of the Heihe basin. In response, the rules for water distribution were established; these rules, and their subsequent revisions (1955–57, 1960, 1962–63, 1966–89, and 2000–06 CE), remain in force today (Inoue et al. 2007). In 1726 CE, the Toryuud people, who led a nomadic existence around Ejina, complained that the rivers dried up during spring and summer. By the 18th century, the population had increased dramatically and the continuing settlement of ex-military personnel had reached its upper limit in terms of water availability. Diatom analysis of lake sediments from Gashun Nor confirm that very little river water flowed into the lake between 1740 and 1900 CE, which coincides with the period of excessive extraction of water for irrigated agriculture in the middle reaches. The monsoon Asia drought atlas (Cook et al. 2010), which is plotted on a scale equal to 2.5° latitude/longitude grids, indicates that the east india drought occurred during 1790, and from 1792 to 1796 CE. The great drought occurred from 1876 to 1878 CE. These droughts adversely affected the harvest in the Hei river basin (Inoue et al. 2007).

The population in present-day Zhangye and Jiuquan is one-fifth of that during the Ming Dynasty, due to the effects of the Dongan Revolt (1862–1877 CE). In the time of the
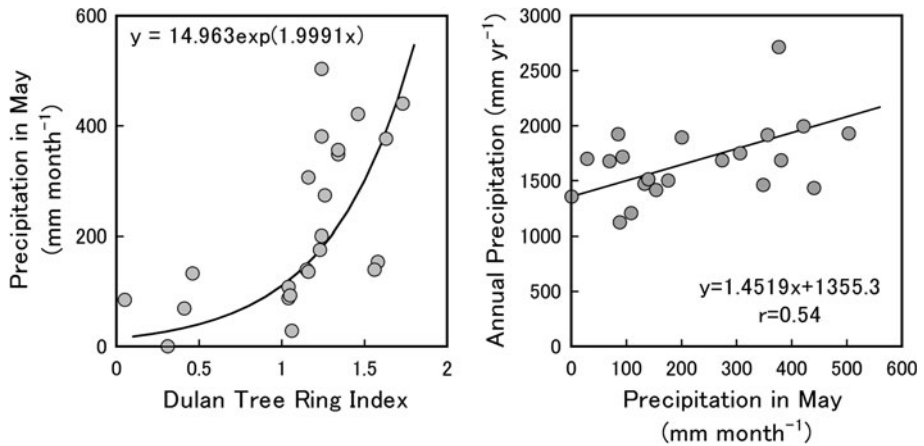
Fig. 4 a Relationship between tree-ring width and precipitation in May at Dulan (35°50'–36°30'N, 97°40'–98°20'E), from 1978 to 2002. **b** The relationship between precipitation in May and annual precipitation at Dulan. Data from Yatagai et al. (2009)

Republic of China (1912 CE–), the population, and the amount of land used for agriculture, has increased dramatically in both the middle and lower reaches, and water from the Beidahe no longer reached the lower section of the basin, plus the lakes Sogo Nor and Gashon Nor had dried up. Because of the sharp increase in both the amount of irrigated agricultural land and the size of the population in the middle and lower reaches, there occurred a sharp decline in groundwater levels and vegetation cover (Kubota 2007). A large flood occurred in the middle to lower reaches in 1930 CE (Endo et al. 2005).

Methods

Meteorological data from the last two millennia

Using multi-proxy data from ice cores, tree-rings, and lake sediments, Yang et al. (2002) reconstructed decadal changes in temperature anomaly data. The annual temperature anomaly is interpolated by assuming linear change. Here, we estimate temperature change based on the differences between the temperature anomaly data of Yang et al. (2002), and temperature data from the NCEP/NCAR (National Centres for Environmental Protection/ National Centre for Atmospheric Research) Reanalysis project for 1980 and 1990 at an altitude of 4,300 m. The temperature at this altitude was calculated from the temperature at 600 hPa and the temperature lapse rate, which was in turn calculated from the temperatures and geopotential heights at 600 and 700 hPa, respectively.

Moisture stress during the growing season is a major limiting factor for tree-ring growth in the arid regions of China. Consequently, variations in tree-ring width can be used as a proxy to reconstruct precipitation amounts during the growing season. Zhang et al. (2003) report a tree-ring width chronology spanning 2326 years obtained from archaeological wood and living trees at Dulan, 300 km from the Hei river basin (35°50'–36°30'N, 97°40'–98°20'E; Fig. 1). The tree-ring indices correlate most strongly with spring precipitation (May–June) ($r = 0.58$, $p < 0.001$, Pearson's correlation coefficient).
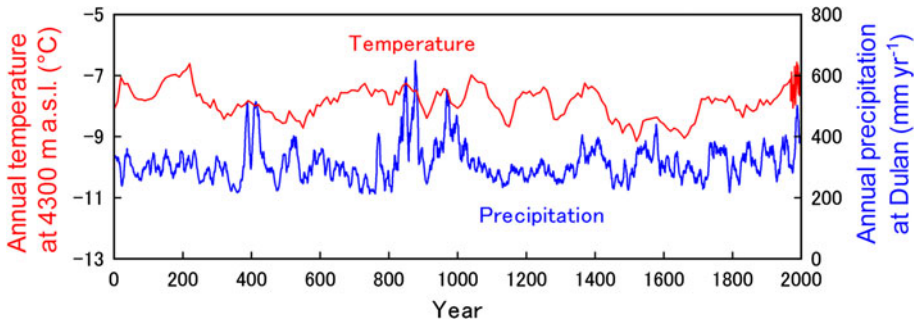
Fig. 5 Annual precipitation at Dulan, calculated from the index of tree-ring width (Zhang et al. 2003). Temperature fluctuations (Yang et al. 2002) are also shown

We analysed the monthly precipitation data (Yatagai et al. 2009) from the tree sampling site at Dulan (36°00′–36°30′N, 97°30′–98°00′E). Precipitation amounts in May, between 1978 and 2002, correlated strongly with tree-ring indices ($n = 25$, $r = 0.61$, $p < 0.01$) (Zhang et al. 2003), as shown in Fig. 4a. We derived the following relationship between precipitation in May (P_{may}) and the tree-ring index (TRI):

$$P_{\mathrm{may}} = 14.963 \times e^{(1.9991\mathrm{TRI})} \tag{1}$$

Precipitation in May also shows a relatively high correlation ($n = 25$, $r = 0.54$, $p < 0.01$) with annual precipitation (P_{yr}), as shown in Fig. 4b, and the equation for this relationship is as follows:

$$P_{\mathrm{yr}} = 1.4519 \times P_{\mathrm{may}} + 135.53 \tag{2}$$

Variations in annual precipitation at Dulan were reconstructed from the TRI using Eqs. (1), (2). Precipitation and temperatures during the last two millennia, as used for our discharge calculation, are shown in Fig. 5.

Areal distribution of precipitation

Monthly precipitation was estimated within each grid square from the monthly precipitation at Dulan (36°00′–36°30′N, 97°30′–98°00′E), and the monthly temperature at 5,000 m a.s.l., by multiple regression analysis. The monthly temperature was estimated using temperatures (NCEP/NCAR reanalysis data) and geopotential heights at 500 and 600 hPa, respectively, assuming a uniform temperature lapse rate.

As for vertical distribution profile of precipitation, Sakai et al. (2010:4) established the vertical distribution profile of daily precipitation at z m altitude from the following equation:

$$P_r(z) = [1 + C(z - z_{\mathrm{b}})]P_{\mathrm{rx}} \tag{3}$$

where $C = 1/1{,}600$ m^{-1}, z_{b} is the average altitude of 0.5° lat/lon grid squares , P_{rx} is the daily precipitation data (Yatagai et al. 2009)

Estimation of daily meteorological data from annual data

Glacier mass balance and discharge models are based on Sakai et al. (2009, 2010), while the glacier mass balance model based on the heat balance method required only daily
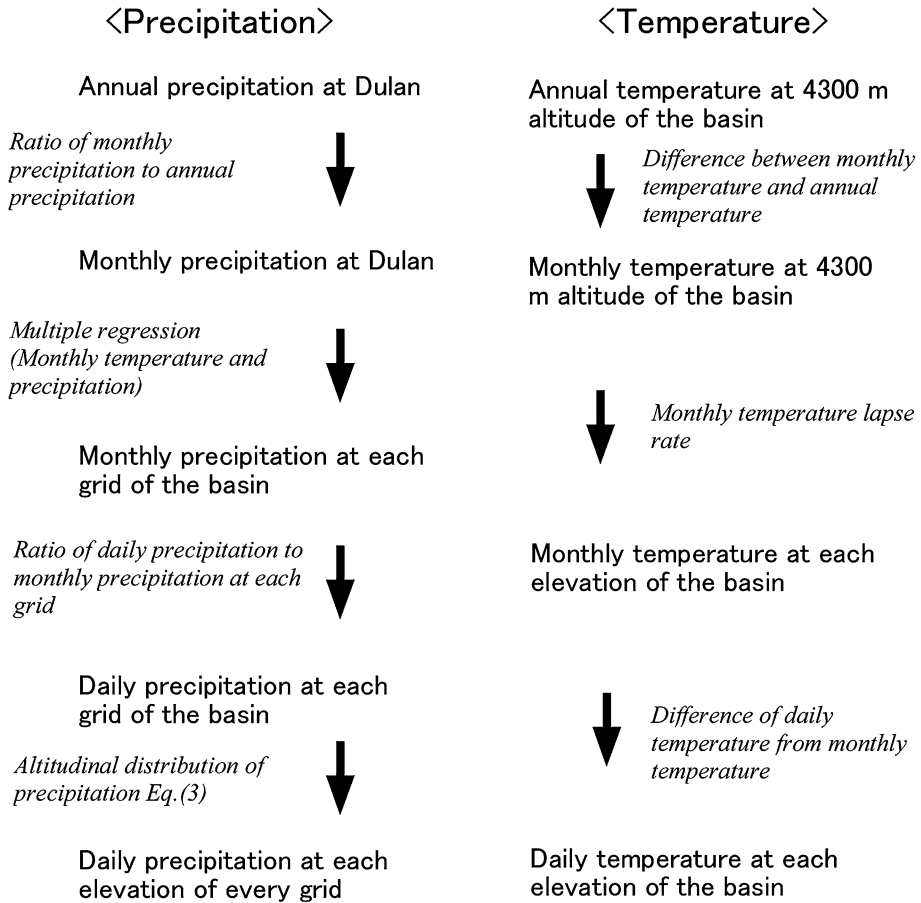
⟨Precipitation⟩

Annual precipitation at Dulan

*Ratio of monthly
precipitation to annual
precipitation*

Monthly precipitation at Dulan

*Multiple regression
(Monthly temperature and
precipitation)*

Monthly precipitation at each
grid of the basin

*Ratio of daily precipitation to
monthly precipitation at each
grid*

Daily precipitation at each
grid of the basin

*Altitudinal distribution of
precipitation Eq.(3)*

Daily precipitation at each
elevation of every grid

⟨Temperature⟩

Annual temperature at 4300 m
altitude of the basin

*Difference between monthly
temperature and annual
temperature*

Monthly temperature at 4300
m altitude of the basin

*Monthly temperature lapse
rate*

Monthly temperature at each
elevation of the basin

*Difference of daily
temperature from monthly
temperature*

Daily temperature at each
elevation of the basin

Fig. 6 Flow chart summarising the procedure used to estimate the daily precipitation amounts, and daily temperatures, in each grid square, using the annual precipitation at Dulan and annual temperature for China, respectively (as shown in Fig. 5)

temperature and data to allow modelling' after precipitation. Annual precipitation data are available for Dulan, and annual temperature data for all of China, for the last two millennia (Fig. 5). However, daily data are required if we are to calculate the fluvioglacial discharge and the mass balance.

Figure 6 shows a procedure for estimating the daily precipitation and temperature within each grid square from the annual precipitation at Dulan, and the annual temperature in China. Here, temperature is assumed to be uniform in the basin, and precipitation is estimated for each 0.5° lat/lon grid square using the precipitation data given by Yatagai et al. (2009) for the period 1978–2002.

We estimated the monthly temperatures and precipitation at Dulan from proxy annual temperature and precipitation data, by assuming that the monthly ratios of precipitation, and the differences in monthly and annual temperature, have been constant over the last 2000 years, which were derived from precipitation data at Dulan (36°00′–36°30′N, 97°30′–98°00′E) for the period 1978–2002 (Yatagai et al. 2009) and the average temperature

NCEP/NCAR Reanalysis data for the period 1978–2000 at 500 and 600 hPa, and the geopotential data at 500 and 600 hPa.

The daily precipitation within each grid square was estimated from the ratio of daily to monthly precipitation in 1978. The daily temperature was similarly estimated from the difference between daily and monthly temperatures in 1978.

Present-day distribution of glaciers and basins

For the three basins studied (Fig. 1b), we established two zones before calculating the discharge from the basin: areas occupied by glaciers (the glacier zone), and the glacier-free zone. A digital elevation model (DEM) was used to analyse the altitudinal area distribution and the position of the glaciers in the three basins. The DEM of the basins was generated from Shuttle Radar Topography Mission (SRTM). In addition, the Advanced Spaceborne Thermal Emission and Reflection radiometer (ASTER). DEM was superimposed on the DEM produced from the SRTM to fill gaps in the SRTM DEM. The maximum difference in the two sets of elevations was 5 m.

The boundary of the drainage area was evaluated by superimposing a map (scale: 1:1,000,000) onto the DEM produced by the ASTER satellite image. The altitudinal area distributions of these basins were derived for intervals of 50 m. The drainage areas of the Yingluoxia, Beidahe, and Hongshuibahe basins are 9983, 5981, and 1569 km^2, respectively.

The glacier zone was extracted by superimposing visible images from the Landsat satellite, taken in the period 1995–2001, and the DEM produced by the ASTER satellite image. As far as possible, we selected Landsat satellite images showing no clouds or seasonal snow. Glaciers with areas <0.01 km^2 could not be detected from the satellite images. The glacier zone areas in the Yingluoxia, Beidahe, and Hongshuibahe basins measure 39, 117, and 111 km^2, respectively. Then, the ratios of the glacier to total drainage area in the Yingluoxia, Beidahe, and Hongshuibahe basins are 0.4, 1.7, and 7.1 %, respectively.

Results

Changes in glacier area

Several researchers (Van de Wal and Wild 2001; Ye et al. 2003; Raper and Braithwate 2006) have developed models that show that the rate of response of a glacier area to climate change depends upon the size of the glacier. Therefore, we grouped glacier areas in the three basins into five size classes within each 0.5° lat/lon grid square, namely: 0.01–0.049, 0.05–0.099, 0.10–0.499, 0.50–0.999, and >1.00 km^2.

We assume that the altitudinal glacier area distribution is rhombic in shape (Fig. 7), based on the lowest and highest altitudes, and the altitude of the maximum glacier area. Given that the interval used in determining the altitudinal glacier area distribution is 50 m, horizontal distance along the length of the glacier, for a vertical drop of 50 m (HD), can be calculated as follows,

$$\text{HD} = \frac{50}{\tan\left(\frac{\beta\pi}{180}\right)} \tag{4}$$

Then, glacier width, W (Fig. 7), at the altitude of the maximum glacier area, can be calculated using glacier slope (β (unit:degree)) as follows.

$$W = \frac{S_{\max}}{HD} \tag{5}$$

The average slope of the July 1st Glacier was 10°. But, we do not know the average inclination of glaciers in the studied basin. Then, we calculated glacier area fluctuations using five slopes 8.0°, 9.7°, 11.3°, 14.0°, and 18.3°.

Glacier area change is assumed to conform to the following pattern. The area of the glacier located at a higher altitude than the maximum glacier area (AMG) is taken to be constant, whereas the area of the glacier below the AMG, and the glacier terminus, changes (see Fig. 7).

Moreover, glacier area is assumed to change with changes in glacier volume, and this relationship can be expressed as follows (Chen and Ohmura 1990; Liu et al. 2003):

$$v = c\alpha^{\gamma} \tag{6}$$

where v is the volume of glacier (m^3), α is the area of glacier (km^2), c is t constant (0.04), and γ is the constant (1.36).

Figure 8 shows the calculated glacier area fluctuation using five slopes and glacier area during the little ice age (LIA) maximum and at present. Calculated glacier area fluctuation with 11.3° inclination corresponded well with the glacier area in the LIA and at present. We can, therefore, assume that the maximum glacier area is a rectangle, with 11.3°
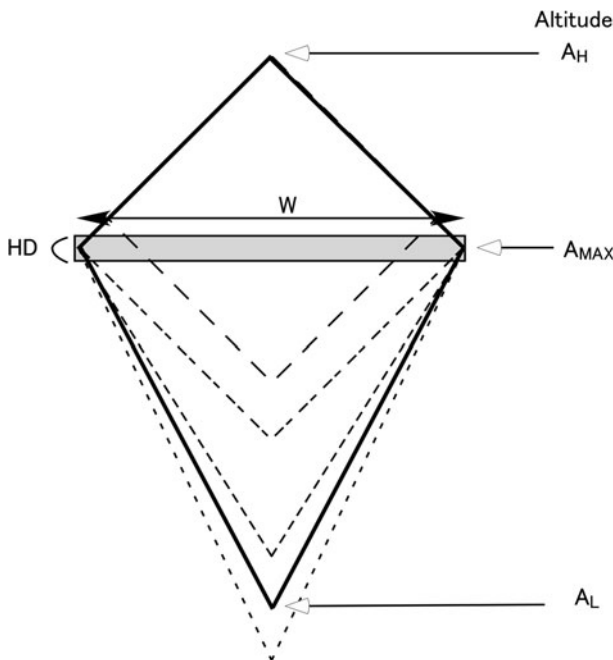
Fig. 7 Schematic representation of the simplified altitudinal glacier area distribution, and glacier area change. HD is the horizontal distance along the length of the glacier, for a vertical drop of 50 m; W is glacier width at each 50 m interval; A_H and A_L are the altitudes of the highest and lowest points of the glacier, respectively, and A_{MAX} is the maximum glacier area. Only those parts of the glacier that are at lower altitudes than the altitude of maximum glacier area (A_{MAX}) show a change in area. Glacier areas are assumed to be rhomboids, which fluctuate in shape as shown
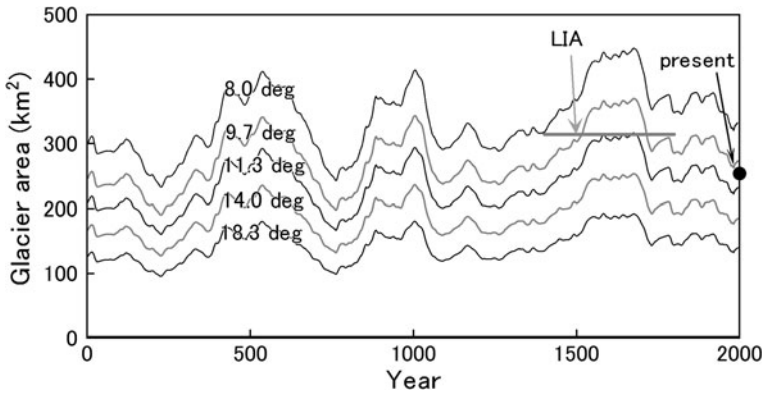
Fig. 8 Calculated glacier area fluctuations for the last 1000 years with 5 inclinations of glacier (8.0, 9.7, 11.3, 14.0, 18.3 degrees). Gray line and black circle indicate the glacier area during the LIA glacier maximum and at present, respectively

Fig. 9 Relation between actual glacier areas extracted from satellite image, and simplified glacier areas that were assumed to have the rhombus shape. Those data were summed at each grid and each glacier area size
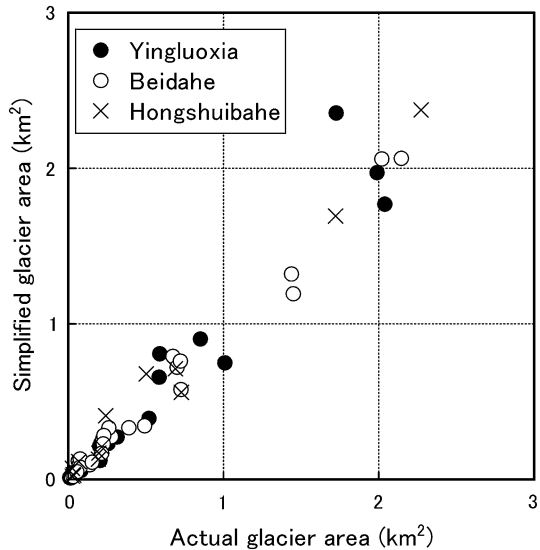
inclination hereafter. The simplified glacier areas with 11.3° in inclination correspond very well with the actual glacier areas (Fig. 9).

Initial glacier area and response times

No empirical data are available regarding the initial glacier area to use in calculating glacier area variations over the last two millennia. Instead, we ran a discharge model using averages values for temperature and precipitation over the last two millennia, and assumed that the initial glacier area was the same as the average value over the last two millennia. Example of calculations were shown in Fig. 10. Therefore, for first several 100 years of the calculation, variations in glacier area are affected by the initial conditions of the model. We discuss the response time of glacier area in the next section. The response time of the five
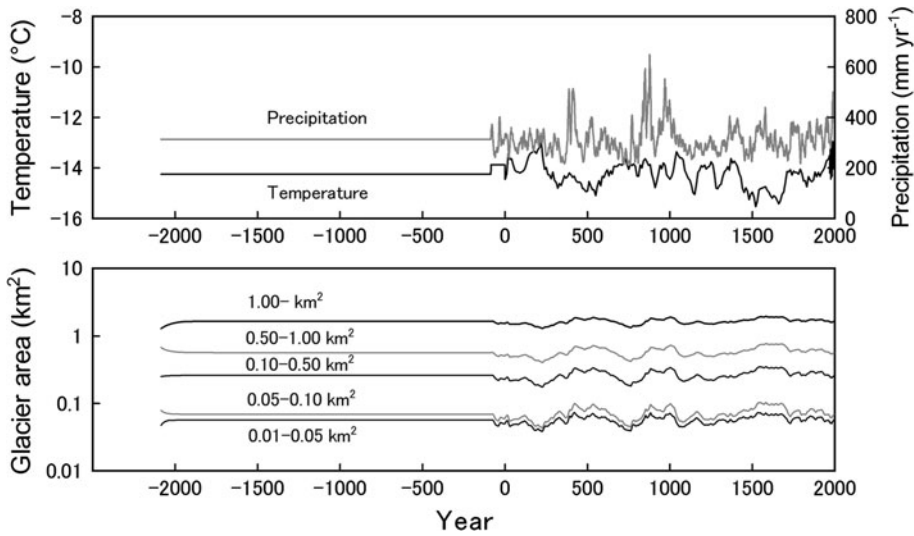
Fig. 10 Example of glacier area calculations for each of the five glacier size classes. See the text for further details
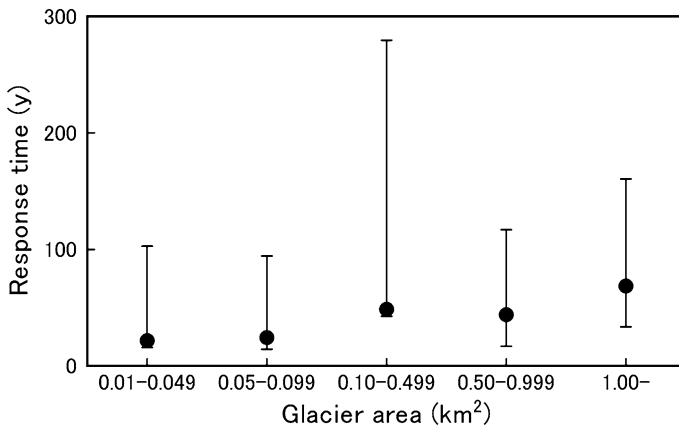

Fig. 11 Response times of the glacier area for each of the five size classes. Error bars indicate the maximum and minimum values of glacier area, calculated for each grid square, and for each of the five size classes

classes of glacier area (Fig. 11) increased with glacier size, so that the response time for small glaciers (0.01–0.49 km^2), averaged over whole grid squares, was ca. 21 years, while it increased to ca. 69 years for relatively large glaciers (>1.00 km^2). With a few exceptions, the response time of the glaciers in each grid square, regardless of glacier size, was on the order of 10^1 y. The calculated maximum response time was 230 years; i.e., much less than two millennia.

Figure 12a shows the variations in temperature and precipitation at Dulan used to calculated the glacier mass balance and discharge from the glacier and glacier-free zones. Figure 12b–d shows the variations in calculated glacier areas, fluvioglacial discharge, and total discharge from each basin.
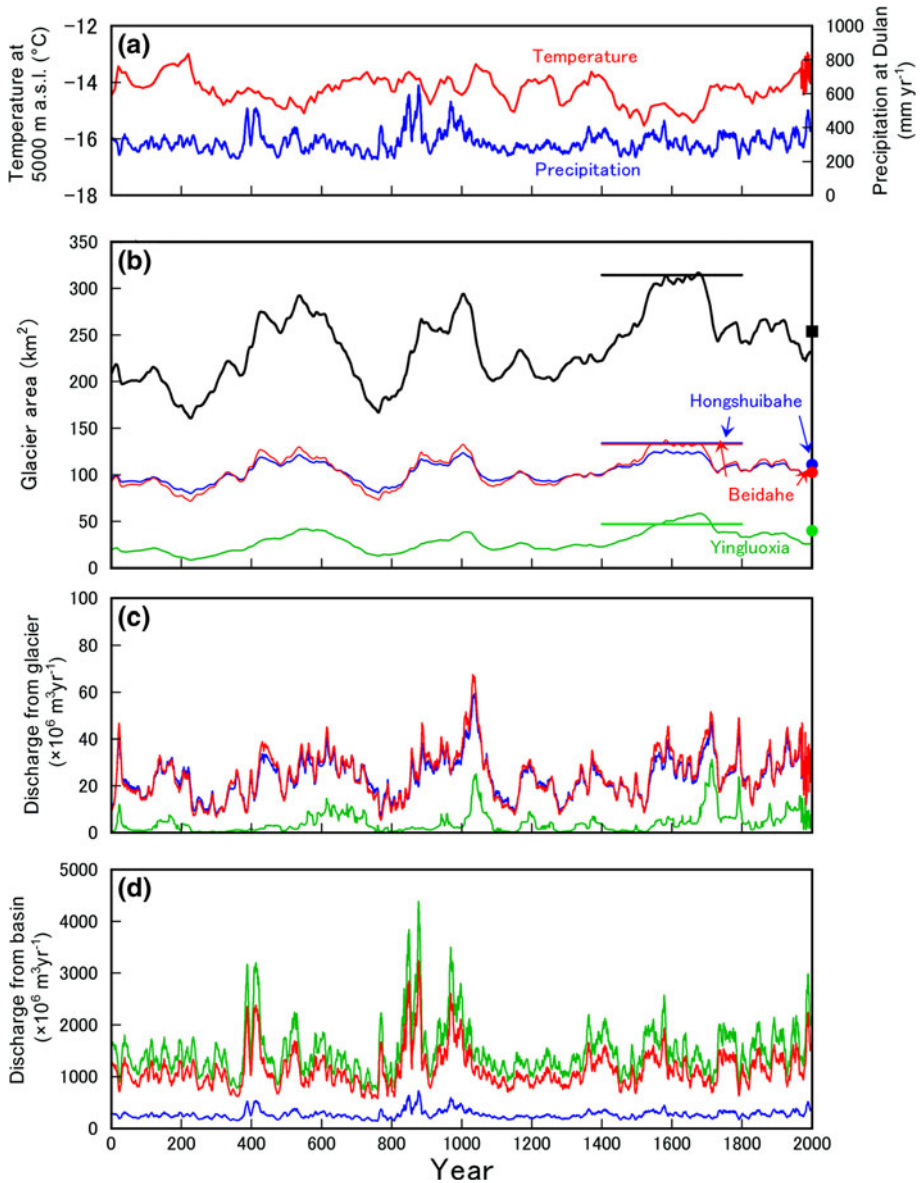
Fig. 12 a Variations in temperature and precipitation used in the calculations. **b** Calculated glacier area fluctuations; horizontal line indicates period of maximum glacier area. **c** Discharge from the glaciers in each basin. **d** Discharge from each basin

Discussion

The maximum response time of the glacier area in this study was 230 years (Fig. 11), so the calculated fluvioglacial discharge and variations in glacier areas during the first few 100 years are affected by the initial glacier area, which was calculated using the average temperature and precipitation over the two millennia. Thus, variations in discharge from

the glacier, and the glacier mass balance calculated for the last two millennia, reflect the meteorological conditions from at least 300 years ago. Hereafter, we discuss on the water environment from 300 CE to present.

Figure 12b shows that the glacier area expanded significantly on three separate occasions, around 500, 1000 and at the end of the 1700s CE. The calculated glacier area reached a maximum from 1520 to 1690 CE, during the LIA. In Europe, the shrinkage of glaciers at the end of the LIA was caused by decreasing precipitation during the winter season (Vincent et al. 2005). Our calculations show that glacier shrinkage in China was caused mainly by an increase in temperature.

The precise timing of the glacial maximum in the Qilian mountains during the last 2000 years has not been determined, but the periods when the glaciers attained their maximum areas are indicated by the horizontal lines in Fig. 12b. The maximum glacier area for each basin has been estimated from the locations of moraines identified on Corona satellite images. The calculated maximum glacier area during the LIA (1520–1690 CE) is the same as the glacier area maximum given by moraine locations. We have no data on the exact timing of the glacial maximum during the LIA. Nevertheless, our calculations of changes in the areas of the glaciers are consistent with the proposition that the glacial area was at a maximum between 1520 and 1690 CE.

On the basis of C-14 dating in the Nyinchintangla and Gongga mountains, and summarising the work of Iwata and Jiao (1993), Zhou et al. (1991), and Su et al. (1992), Grove (2001) suggested that a glacier advance took place between 1000 and 1200 CE, and then again from late 1200s to early 1400s CE. Our calculations of variations in glacier area (Fig. 12b) are consistent with a glacier advance starting around 1200 CE, although we note that there are no C-14 data from glacial moraines in the Qilian Shan. Our data also correlate well with the glacier advances determined from moraines and C-14 analyses, and this suggests that our approach is both valid and useful.

The average fluvioglacial discharge during the last two millennia in the Yingluoxia, Beidahe, and Hongshuibahe basins was only 0.3, 2.3, and 9.3 %, respectively, of the total runoff of each basin, as the glacier area covered only 1.4 % of the whole basin. The calculated variation in total discharge from the basins was controlled by variations in precipitation. Similarly, Collins (2008) observed discharge in the Swiss Alps and demonstrated that a relatively low glacier area percentage may affect discharge.

The fluvioglacial discharge was relatively small when the glacier area was increasing. In particular, there was no fluvioglacial discharge in the Yingluoxia basin around 300, 1300, and 1500 CE. In contrast, abrupt temperature increases immediately after an expansion of glaciers may cause an increase in discharge, such as occurred in 1038–1714 CE.

No empirical data on glacier discharge are available with which to test our model. However, our calculated changes in glacier area correlate well with direct measurements of the same changes in area. Therefore, our confidence in the calculated discharges from glaciers and basins is high, since glacier mass is calculated from residual precipitation, discharge, and evaporation. That is, the calculated discharges from glaciers and basins are indirectly validated by changes in glacier area.

We compared our calculated dischargers with historical records from each of the Chinese Dynasties. Figure 3 summarises the calculated discharge from the mountain area, the proportion of discharge from the glacier, agriculture activity in the middle and lower reaches (Nakawo 2011), and the area of terminal lakes in the lower reaches.

Inoue et al. (2007) present a summary, taken from historical documents, of drought events in the more heavily populated middle and lower reaches of the Hei river basin. For the Wei, Jin, and the southern and northern Dynasties (220–589 CE), the calculated

discharge from the mountain area followed a decreasing trend from 300 to 360 CE, which may have influenced the aridification of the Juyan delta. For the four droughts along the Hexi Corridor in this period (271, 369, 399, and 405 CE), our calculations coincided with those in 369, 399, and 405 CE. The historical drought on the Mongol plateau (685–687 CE) during the Tang Dynasty (618–907 CE) coincided with low calculated discharges from the mountain area during 686–691 CE. During the Sung period (960–1279 CE), the yearly floods recorded in the 'Dafo-si' temple do not correspond with our calculated total discharges from the mountain areas, as these were low. However, calculated discharges from glaciers increased dramatically from 1153 to 1178 CE, caused by glacier mass shrinkage. Such melt water may have caused flooding, as the melting season is concentrated during the summer months.

During the Yuan period (1271–1368 CE), our calculated low discharges coincide with the recorded droughts at Gansu in 1288 CE, and at Ejina in 1299 and 1331 CE. Subsequently, in both the Ming (1368–1644 CE) and the Qing (1644–1912 CE) periods, many droughts and floods have been recorded. Khara Khoto and Lücheng, which developed old city in the old Juyan delta, have declined between 1413 and 1475 CE. It was caused not only by a change in the course of the river channel from the Juyan delta to the Ejina delta (Endo et al. 2005), but by reduced inflow from mountain areas (1410–1450 CE, Fig. 3), because Gashun Nor also dried up between 1440 and 1530 CE (Endo et al. 2005). The Ejina delta developed during a flood in the period 1350–1400 CE, which coincides with the relatively large calculated discharge from the mountains between 1355 and 1430 CE. The struggle for water in the early 18th century is confirmed by the lower calculated discharge from the mountain areas from 1710 to 1720 CE. The great drought from 1876 to 1878 CE is also apparent in our calculations. During the Republic of China (1912 CE), the calculated discharge from the mountain area has followed a decreasing trend. The flood in 1930 CE was probably not caused by discharge from the mountain area, as this was relatively low at that time. However, the calculated glacier meltwater peaked then, and the flood may have been caused by this concentrated discharge during the summer, which was exacerbated by the dry land maximising runoff.

Figure 13 shows the calculated variations in discharge from the upper reaches of the Hei river basin (Yingluoxia, Beidahe, and Hongshuibahe basins), as well as drought events, for
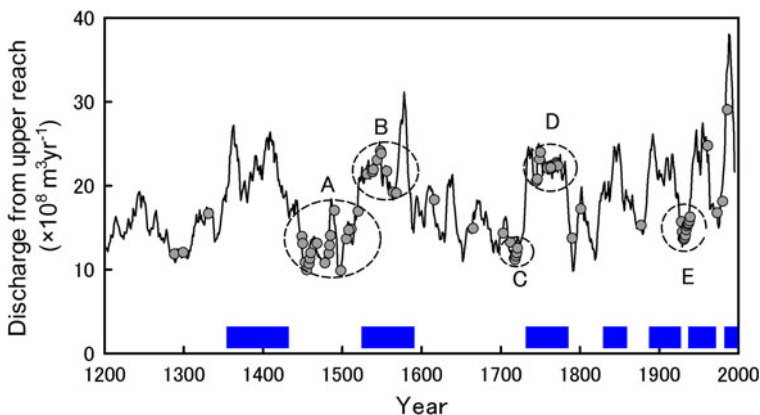

Fig. 13 Five-year moving average of calculated discharge from the entire basin, and five sequential drought events (A–E) recorded in historical documents. The blue bar shows periods with a relatively large discharge

Table 1 Sequence of drought events recorded in historical documents, and calculated relative amounts of discharge from the mountain area

	AD	Calculated discharge with reconstructed temperature and precipitation
A	1449–1520	Little
B	1531–1556	Large
C	1717–1721	Little
D	1749–1772	Large
E	1928–1939	Little

the period 1200–2000 CE (there is a relatively large number of historical documents for this period). We selected only long-lived drought events, which continued intermittently for periods of several years to a few decades, and these events are summarised in Table 1. The calculated discharges during drought events A, C, and E (see Table 1) are relatively small; consequently, we are confident that these droughts were climate driven. In contrast, the calculated discharges during drought events B and D are relatively large (Table 1). These drought events may be attributable to human activity, rather than climatic factors, and might have been caused, for example, by the excessive extraction of river water for irrigation. Indeed, in this region, the pioneering phase of agricultural land-use started in the 14th century (Fig. 3), supporting this interpretation. Clearly, these droughts must be investigated further to determine whether they are simply artefacts of the excessive use of water in the middle reaches.

In Fig. 13, seven long (>10 years) discharge periods are shown from 1200 CE to the present-day (1355–1425, 1525–1585, 1735–1785, 1825–1855, 1885–1925, 1940–1965, and 1980–1995 CE). Four of these periods (1525–1585, 1735–1785, 1940–1965, and 1980–1995 CE) have drought records, while the other three (1355–1425, 1825–1855, and 1885–1925 CE) do not. Between 1355 and 1425 CE, agricultural land-use had not begun (Fig. 3); therefore, human-induced drought could not have occurred because there was a plentiful supply of natural water. The periods 1825–1855 and 1885–1925 CE coincided with Dongan Revolt, and agricultural land was left uncultivated. Therefore, irrigation demands were reduced during these periods, and water shortages did not occur. In this way, the calculated continuous water discharge from the upper reaches can be used to estimate the nature of continuous change in the water environment by taking into account historical events.

Conclusions

We applied the discharge calculation method, established by Sakai et al. (2010), to the Beidahe and Hongshuibahe basins, using proxy temperature and precipitation data, and have been able to reconstruct variations in discharge over the last two millennia. However, we have not been able to validate these calculated variations in discharge with direct observations.

We calculated discharges over the past two millennia using a method that enabled us to calculate both the glacier mass balance, and the fluvial and fluvioglacial discharge from the mountains (Sakai et al. 2010). The total maximum glacier area, estimated from the location of moraines, correlates well with the calculated maximum glacier area from 1500 to the end of the 1700s CE, giving us confidence in the validity of our calculated figures for glacier mass balance. The calculated variations in glacier area indicate that the glacial

maximum occurred between 1520 and 1690 CE. Given that these calculated changes in glacier area appear valid, we can also express confidence in our calculations of fluctuations in discharge from the glaciers and basins.

Migration of river channels has led to changes in the size and location of the terminal lakes, which has significantly affected the water environment in this arid region. In the age of Yuan (1271–1368 CE), sophisticated farming methods, including the recycling of irrigation water, were employed on the old Juyan delta in an attempt to adapt to the shortage of water at that time.

A comparison of discharge from mountains with historical records indicates that some droughts corresponded to a decline in discharge from the mountains, and some floods corresponded to large discharges from the mountains or glaciers.

We also compared calculated fluctuations in discharge with the timing of drought events recorded in historical documents. To ensure the reliability of the data, only multi-year drought events were considered. Some of the historical drought events correlate well with abrupt declines in discharge, as calculated in the present study. Such correlations provide strong evidence for a significant, and real, dry climatic event. In contrast, other historical drought events do not correlate well with our calculated discharges. In such cases, it is possible that the historical drought record is an artefact of an excessive use of water for irrigation in the middle reaches, as for example in the case of the 14th century period of pioneering land-use. By considering not only drought records and the historical background, but also variations in the calculated discharge from the mountains, the continuous variability of the water environment can be estimated even for those periods when no drought records exist.

References

Chen J, Ohmura A (1990) Estimation of alpine glacier water resources and their change since 1870s. IAHS Publ 193:127–135

Collins DN (2008) Climatic warming, glacier recession and runoff from Alpine basins after the little ice age maximum. Ann Glaciol 48:119–124

Cook ER, Anchukaitis KJ, Buckley BM, D'Arrigo RD, Jacoby GC, Wright WE (2010) Asian monsoon failure and megadrought during the last millennium. Science 328(5977):486–489. doi:10.1126/science.1185188

Endo K, Sohma H, Mu G, Qi W, Hori K, Murata T, Zheng X (2005) Paleoenvironment and migration of rivers, delta and lakes in the lowest reaches of Heihe. Project report on an Oasis-region (Research Institute for Humanity and Nature) 5(2):161–171

Endo K, Qi W, Mu G, Zheng X, Murata T, Hori K, Sohma H, Takada M (2007) Change of desert environment and human activities during the last 3000 years in the lowest reaches of Heihe river, China (in Japanese). Project report on an Oasis-region. (Research Institute for Humanity and Nature) 6(2):181–199

Greuell W (1992) Hintereisferner, Austria: mass-balance reconstruction and numerical modelling of the historical length variations. J Glaciol 38(129):233–244

Grove JM (2001) The little ice age. Ancient and modern, vol I, 2nd edn. Taylor & Francis Group, London, New York

Inoue M, Kato Y, Moriya K (eds) (2007) Regional history in oasis regions. Shoukado, Kyoto

Iwata S, Jiao K (1993) Fluctuation of the Zepu glacier in late holocene epoch, the eastern Nyanqentanglha mountains, Qing-Zang (Tibet) plateau. In: Yao TD, Ageta Y (eds) Glaciological climate and environment on Qing-Zang plateau. Science Press, Beijing

Kang E, Cheng G, Lan Y, Jin H (1999) A model for simulating the response of runoff from the mountainous watersheds of inland river basins in the arid area of northwest China to climatic changes. Sci China Ser D 42:52–63

Kubota (2007) Nature and water use at Hei river basin. In: Nakawo et al (eds) Half a century of Chinese frontier region. Toho Press, Tokyo

Linderholm HW, Jansson P (2007) Proxy data reconstructions of the Storglaciären (Sweden) mass-balance record back to AD1500 on annual to decadal timescales. Ann Glaciol 46:261–267

Liu S, Sun W, Shen Y, Li G (2003) Glacier changes since the little ice age maximum in the western Qilian Shan, northwest China, and consequences of glacier runoff for water supply. J Glaciol 49(164): 117–124

Mischke S (2001) Mid and late holocene paleoenvironment of the lakes eastern Juyanze and Sogo Nur in NW China, based on Ostracod species assemblages and shell chemistry. Berl Geowiss Abh 35:134

Nakawo M (2011) History and environment at oasis region. Bensey Publishing Inc., Tokyo (in Japanese)

Oerlmans J (1997) A flowline model for Nigardsbreen, Norway: projection of future glacier length based on dynamic calibration with the historic record. Ann Glaciol 24:382–389

Raper SCB, Braithwate RJ (2006) Low sea level projections from mountain glaciers and icecaps under global warming. Nature 439. doi:10.1038

Raper SCB, Briffa KR, Wigley TML (1996) Glacier change in northern Sweden from AD500: a simple geometric model of Storglaciären. J Glaciol 42(141):341–351

Sakai A, Fujita K, Nakawo M, Yao T (2009) Simplification of heat balance calculation and its application to the glacier runoff from the July 1st glacier in northwest China since the 1930s. Hydrol Process 23(4):585–596. doi:10.1002/hyp.7187

Sakai A, Fujita K, Narama C, Kubota J, Nakawo M, Yao T (2010) Reconstructions of annual discharge and glacier ELA at Qilian mountains in northwest China from 1978 to 2002. Hydrol Process. doi: 10.1002/hyp.7700

Schmeits MJ, Oerlemans J (1997) Simulation of the historical variations in length of unterer Grindelwaldgletscher, Switzerland. J Glaciol 43(143):152–164

Smedt DB, Pattyn F (2003) Numerical modelling of historical front variations and dynamic response of sofiysky glacier, Altai mountains, Russia. Ann Glaciol 37:143–149

Sohma H and 5 others (2007) Environmental change indicating the remains at lower reaches of the Heihe region (Japanese with English abstract). Project Report on an Oasis-region (Research Institute for Humanity and Nature) 6(2):107–121

Su Z, Liu S, Wang N, Shi A (1992) Recent fluctuation of glaciers in the Gongga mountains. Ann Glaciol 16:163–167

Van de Wal RSW, Wild M (2001) Modelling the response of glaciers to climate change by applying volume–area scaling in combination with a high resolution GCM. Clim Dyn 18:359–366

Vincent C, Le Meur E, Six D, Funk M (2005) Solving the paradox of the end of the little ice age in the Alps. Geophys Res Lett 32(9):L09706. doi:10.1029/2005GL022552

Wang G, Cheng G (1999) Water resource development and its influence on the environment in arid zones of China—the case of the Hei river basin. J Arid Environ 43:121–131

Yamaguchi S, Naruse R, Shiraiwa T (2008) Climate reconstruction since the little ice age by modelling Koryto glacier in Kamuchatka Peninsula, Russia. J Glaciol 54(184):125–130

Yang B, Braeuning A, Johnson KR, Shi YF (2002) General characteristics of temperature variation in China during the last two millennia. Geophys Res Lett 29(9). doi:10.1029/2001GL014485

Yatagai A, Arakawa O, Kamiguchi K, Kawamoto H, Nodzu MI, Hamada A (2009) A 44-year daily gridded precipitation dataset for Asia based on a dense network of rain gauges. SOLA 5:137–140. doi: 10.2151/sola.2009-035

Ye B, Ding Y, Liu F, Liu C (2003) Responses of various-sized alpine glaciers and runoff to climatic change. J Glaciol 49(164):1–7

Zhang QB, Cheng G, Yao T, Kang X, Huang J (2003) A 2,326-year tree-ring record of climate variability on the northern Qinghai-Tibetan plateau. Geophys Res Lett 30(14):1739. doi:10.1029/2003GL017425

Zhou SZ, Chen FH, Pan BT, Cao JX, Li JJ, Derbyshire E (1991) Environmental change during the holocene in western China on a millennial timescale. The Holocene 1:151–156

Zuo Z, Oerlemans J (1997) Numerical modeling of the historic front variation and the future behaviour of the Pasterze glacier, Austria. Ann Glaciol 24:234–241

Author Biographies

Akiko Sakai is an assistant professor in the Nagoya University in Japan. Her subject is glacial lake and discharge from glacier based on the field observation in Asia.

Mitsuyuki Inoue is an Associate Professor in Ritsumeikan University. His subject is Oriental History. And he especially interested in the society and culture in late imperial China.

Koji Fujita is an Associate Professor at the Graduate School of Environmental Studies, Nagoya University. His research has focused on fluctuations of Himalayan glaciers, ice-core based paleoclimate reconstruction in the Asian highlands, and stable water isotope climatology in Antarctica.

Chiyuki Narama is a project researcher in RIHN (Research Institute for Humanity and Nature) in Kyoto, Japan. His subject is glacial geomorphology and glacier hazards in Central Asia and Himalayas.

Jumpei Kubota is a professor in RIHN. His subject is hydrology. He has been conducting a transdiciplinary research project in Central Asia, focusing on the historical intaraction between human activities and the environment.

Masayoshi Nakawo is Executive Director in National Institutes for the Humanities in Japan. His subject has been Earth Sciences. And now he also works on the historical document and ethnology.

Tandong Yao is the president of Institute of Tibet Plateau Research, Chinese Academy of Science in China. His major subject is glaciology.